Evaluating the NMME-2 system prediction skill for springtime ENSO phase evolution and its relation to tornado outbreaks in the U.S.

A Joint Proposal from the
University of Miami/Cooperative Institute for Marine and Atmospheric Studies,
NOAA/Atlantic Oceanographic and Meteorological Laboratory,

To the
NOAA/CPO MAPP (Competition–6) North American Multi-Model Ensemble system evaluation and application: Area-A and -B

By

Sang-Ki Lee[1, 2], Robert Atlas[2], and Chunzai Wang[2]
In collaboration with Scott Weaver[3]

[1] Cooperative Institute for Marine and Atmospheric Studies
University of Miami
4600 Rickenbacker Causeway
Miami, FL 33149

[2]Atlantic Oceanographic and Meteorological Laboratory, NOAA
4301 Rickenbacker Causeway
Miami, FL 33149

[3]Climate Prediction Center, NOAA
5830 University Research Court
College Park, MD 20740

Funding Opportunity #: NOAA-OAR-CPO-2015-2004099
CFDA #: 11.431
Competition ID (for MAPP): 2488571

Proposed Start Date: September 1, 2015

Budget	(Year 1)	(Total)
(CIMAS)	$69.6K	$69.0K
(Total)	$69.0K	$69.0K

Institutional Representative
Bonnie Townsend
4600 Rickenbacker Causeway
Miami, FL 33149
Phone: 305-421-4084; Email: b.townsend@miami.edu

Lead-PI: Sang-Ki Lee
Phone: 305-361-4521; Fax: 305-361-4412; Email: sang-ki.lee@noaa.gov

Evaluating the NMME-2 system prediction skill for springtime ENSO phase evolution and its relation to tornado outbreaks in the U.S.

Institutions: University of Miami/CIMAS and NOAA/AOML
Principal Investigator: S.-K. Lee (Lead PI), R. M. Atlas and C. Wang
Budget Period: September 1, 2015 to August 31, 2016 (1 year)
Total Proposed Cost: $69.0K

Abstract

The record-breaking U.S. tornado outbreak in the spring of 2011 prompts the need to identify and understand long-term climate signals that may provide seasonal predictability for intense tornado outbreaks. Currently, seasonal forecast skill for intense U.S. tornado outbreaks, such as occurred in 2011, has not been demonstrated. A recent study by Lee et al. [2013] used both observations and modeling experiments to find that a positive phase of the Trans-Niño (TNI), characterized by cooling in the central tropical Pacific and warming in eastern tropical Pacific, is associated with large-scale processes that may contribute to major tornado outbreaks over the U.S. In particular, they found that seven of the ten most active tornado years during 1950 – 2010, including the top three, are characterized by a strongly positive phase of the TNI, suggesting that if we can predict the TNI, we may be able to issue a seasonal warning (or outlook) for extreme tornado outbreaks over the U.S.

The North American Multi Model Ensemble Phase 2 (NMME-2) system is a global, fully coupled multi-model ensemble forecast system, currently consisting of nine models from six institutes, and show improved performance over a single model in predicting ENSO indices and U.S. rainfall variability [Kirtman et a., 2014]. The main goal of this proposal is to understand the skill and limitations of the NMME-2 system in predicting the springtime ENSO phase evolution and other key regional parameters for the U.S. tornado outbreaks in March-April-May (MAM, the peak of the tornado season) with 1 to 3 months of lead-time (i.e., January, February, and March initializations). To achieve this goal, our work will be comprised of three tasks: (task-1) evaluate the NMME-2 prediction skill for springtime ENSO phase evolution and its relation to U.S. tornadic environments; (task-2) construct proxy tornado indices using the NMME-2 analysis; (task-3) analyze the NMME-2 prediction skill for the occurrence of U.S. tornado outbreaks. Successfully completing these three tasks may lead to development of a skillful seasonal outlook for U.S. tornado outbreaks based on the NMME-2 system.

The proposed work contributes directly to NOAA CPO FY2015 MAPP funding Competition-6, Area-A Evaluation of NMME system predictions: “Proposed NMME evaluations will examine the skill of NMME system predictions focusing on less well documented, yet potentially important aspects of the predictions. Of particular interest are those studies evaluating the prediction of large-scale, extended lead time conditions conducive to extremes such as heat waves, extreme precipitation (rain, snow or ice storms) or droughts provided a theoretical basis for expecting predictability on ISI timescales exists.” and Area-B Exploration of new applications of NMME system predictions: “Application of the NMME for the development of new prediction products may be proposed as part of exploratory pilot studies.” This proposed work will be conducted under the auspices of the CIMAS at the University of Miami’s RSMAS, and addresses CIMAS Theme: (Climate Research and Impacts). This work is relevant to the NOAA goals: (Weather-Ready Nation: Society is prepared for and responds to weather-related events, and Climate Adaptation and Mitigation: An informed society anticipating and responding to climate and its impacts) in support of NOAA’s Strategic Plan.

Results from Prior NOAA CPO Support (Last Three Years)

(1) NOAA/CPO MAPP Program: Toward developing a seasonal outlook for the occurrence of major U. S. tornado outbreaks, PIs: S.-K. Lee, R. Atlas, C. Wang, D. B. Enfield, and S. Weaver, $430.0K, August 1, 2012 to July 31, 2015.

The main goal of this project is to explore long-term climate signals that may potentially provide seasonal predictability of U.S tornado activity. Through this project, we have identified an optimal ENSO pattern that enhances large-scale atmospheric processes conducive to major tornado outbreaks in the U.S. Lee et al. [2013] that summarized this finding was highlighted in Feb, 2013 issue of Bulletin of the American Meteorological Society as Paper in Note. Currently, our research focus is to objectively characterize the springtime ENSO phase evolution and its relationship with rainfall and tornado activity in the continental U.S. Three papers (two published and one in revision) directly resulted from this project are listed below.

Lee, S.-K., R. Atlas, D. B. Enfield, C. Wang and H. Liu, 2013: Is there an optimal ENSO pattern that enhances large-scale atmospheric processes conducive to major tornado outbreaks in the U.S.? J. Climate, 26, 1626-1642. doi:http://dx.doi.org/10.1175/JCLI-D-12-00128.1.

Lee, S.-K., B. E. Mapes, C. Wang, D. B. Enfield and S. J. Weaver, 2014: Springtime ENSO phase evolution and its relation to rainfall in the continental U.S. Geophys. Res. Lett., 41, 1673-1680. doi:10.1002/2013GL059137.

Lee, S.-K. P. N. DiNezio, E.-S. Chung, S.-W. Yeh, A. T. Wittenberg, and C. Wang, 2014: Spring persistence, transition and resurgence of ENSO. Geophys. Res. Lett., In-revision.

(2) NOAA/CPO MAPP Program: Variability and predictability of the Atlantic warm pool and its impacts on extreme events in North America, PIs: C. Wang, S.-K. Lee and D. B. Enfield, $442.2K, August 1, 2012 to July 31, 2015.

This project is to study the Atlantic warm pool (AWP) and its impact on climate variability in North America. Our research supported by this project has resulted in ten publications, six of which are listed below.

Lee, S.-K., C. R. Mechoso, C. Wang, and J. D. Neelin, 2013: Interhemispheric influence of the northern summer monsoons on the southern subtropical anticyclones. *J. Climate*, 26, 10193-10204.

Liu, H., C. Wang, S.-K. Lee, and D. B. Enfield, 2013: Atlantic warm pool variability in the CMIP5 simulations. *J. Climate*, 26, 5315-5336.

Liu, H., C. Wang, S.-K. Lee, and D. B. Enfield, 2014: Inhomogeneous influence of the Atlantic warm pool on United States precipitation. *Atmos. Sci. Lett.*, in press.

Wang, C., L. Zhang, S.-K. Lee., L. Wu, and C. R. Mechoso, 2014: A global perspective on CMIP5 climate model biases. *Nature Climate Change*, 4, 201-205.

Zhang, L., and C. Wang, 2013: Multidecadal North Atlantic sea surface temperature and Atlantic meridional overturning circulation variability in CMIP5 historical simulations. *J. Geophys. Res.*, 118, 5772–5791.

Zhang, L., C. Wang, and S.-K. Lee, 2014: Potential role of Atlantic warm pool-induced freshwater forcing in the Atlantic meridional overturning circulation: Ocean-sea ice model simulations. *Clim. Dyn.*, 43, 553-574.

Statement of Work

1. Introduction

The need for increased understanding of regional climate variability and change has recently been elevated within the national and international climate science communities. Among the many facets of this framework is the further refinement and characterization of the linkage between extremes of weather and climate. Indeed, the societal impacts of climate variability and change are typically communicated through the weather timescale. As such, placing extreme weather phenomena in a climate context can further our scientific understanding and prediction of the characteristics of the weather-climate linkage.

In April and May of 2011, a record breaking 1,243 tornadoes were reported in the U.S., of which 1,061 were confirmed by the Storm Prediction Center (SPC). The SPC provided adequate warnings several days in advance of these major tornado outbreak episodes, which undoubtedly saved lives. Nevertheless, these extreme outbreak episodes have caused devastating societal impacts with 517 tornado-related fatalities, making 2011 one of the deadliest tornado years in U.S. history [http://www.spc.noaa.gov/climo/torn/STATIJ11.txt]. The series of extreme U.S. tornado outbreaks in 2011 prompt the need to identify and understand long-term climate signals that could potentially provide seasonal predictability for intense tornado outbreaks over the U.S.

To some extent, the seasonal climate variability over North America is linked with phases of the El Niño Southern Oscillation (ENSO) [e.g., Ropelewski and Halpert 1987]. Variations in the location of tropical heating anomalies associated with ENSO modulate the general atmospheric circulation over the U.S., providing the background environment for climatic anomalies. This linkage is strongest during the boreal winter, however, the atmospheric response may persist well into the following spring [e.g., Hoerling and Kumar 1997; Kumar and Hoerling 2003; Ding et al. 2011]. Previous studies have investigated the ENSO linkages of annual U.S. tornadic activity to traditional ENSO indices [Marzaban and Schaeffer 2001], and wintertime tornado outbreaks [Cook and Schaefer 2008]. These studies characterized the correlation between ENSO and U.S tornadoes as very weak.

Lee et al. [2013] used both observations and modeling experiments to confirm the very weak connectivity between conventional ENSO indices and U.S. tornado activity. However, they found that a positive phase of Trans-Niño index (TNI) [Trenberth and Stepaniak 2001], characterized by cooling in the central tropical Pacific (CP) and warming in the eastern tropical Pacific (EP), is much more strongly linked to increased tornado activity over the U.S. than the traditional ENSO indicators in spring. A further study by Weaver et al. [2012] confirmed this finding and added that a positive phase of the TNI is linked to the eastward shift of the North American low-level jet (NALLJ) and associated increase in tornado activity over the Southeastern U.S.

A recent study showed that the springtime ENSO phase evolution is better represented by the TNI index than the conventional ENSO indices [Lee et al., 2014], which explains at least partially why the U.S. tornado activity in spring is more strongly linked to the TNI. Nevertheless, the TNI explains only about 10% of the total variance in the number of intense (i.e., from F3 to F5 in the Fujita-Pearson scale) U.S. tornadoes in spring. Thus, the seasonal predictability, which can be defined as a ratio of the climate signal (the TNI index in this case) to the atmospheric noise signal, is low [Lee et al. 2013]. Nevertheless, seven of the ten most active U.S. tornado years during 1950-2010 including the top three years are characterized by a strongly positive phase of the TNI [Lee et al. 2013]. This suggests that if we can predict the TNI, we may be able to issue a seasonal warning (or outlook) for extreme tornado outbreaks over the U.S.

2. Background

2.1 *Large-scale atmospheric processes conducive to major tornado outbreaks in the U.S*

In the U.S. east of the Rocky Mountains, cold and dry upper-level air from the high latitudes often converges with warm and moist lower-level air coming from the Gulf of Mexico (GoM). Due to this so-called large-scale differential advection (i.e., any vertical variation of the horizontal advection of heat and moisture that decreases the vertical stability of the air column [Whitney and Miller, 1956]), conditionally unstable atmosphere with high convective available potential energy (CAPE) is formed. Additionally, the low-level vertical wind shear associated with the upper-level westerly and lower-level southeasterly (i.e., wind speed increasing and wind direction changing with height) provides the spinning effect required to form a horizontal vortex tube. The axis of this horizontal vortex tube can be tilted to the vertical by updrafts and downdrafts to form an intense rotating thunderstorm known as a supercell, which is the storm type most apt to spawn intense tornadoes [e.g., Doswell and Bosart, 2001]. Consistently, both the moisture transport from the GoM to the U.S. and the low-level vertical wind shear in the central and eastern U.S. are positively correlated (above 95% significance level) with the number of intense U.S. tornadoes in April and May (AM) as shown in Table 1.

Table 1. Correlation coefficients of various long-term climate patterns in December-February (DJF), February-April (FMA), and April and May (AM) with the number of intense (F3 - F5) tornadoes in AM during 1950-2010. All indices including the tornado index are detrended using a simple least squares linear regression. The SWD, ERSST3, and NCEP-NCAR reanalysis are used to obtain the long-term climate indices used in this table. Correlation coefficients above the 95% significance are in bold. See Lee et al. [2013] for more detail.

Index	DJF	FMA	AM
Gulf-to-U.S. moisture transport	0.08	0.20	**0.40**
Low-level vertical wind shear	0.12	0.20	**0.44**
GoM SST	0.15	0.21	0.20
Niño-4	-0.22	-0.20	-0.19
Niño-3.4	-0.13	-0.13	-0.11
Niño-1+2	0.02	0.11	0.15
TNI	**0.28**	**0.29**	**0.33**
PNA	-0.05	-0.10	-0.20
PDO	-0.12	-0.10	-0.14
NAO	-0.01	-0.10	-0.18

The Pacific - North American (PNA) pattern in boreal winter and spring is linked to the large-scale differential advection and the lower-level vertical wind shear in the central and eastern U.S. as discussed in earlier studies [e.g., Munoz and Enfield, 2011]. During a negative phase of the PNA, an anomalous cyclone is formed over North America that brings more cold and dry upper-level air from the high latitudes to the U.S., and an anomalous anticyclone is formed over the southeastern seaboard that increases the southwesterly wind from the GoM to the U.S., thus enhancing the Gulf-to-U.S. moisture transport. Additionally, the lower-level vertical wind shear is increased over the U.S. during a negative phase of the PNA due to the increased upper-level westerly and lower-level southeasterly. Although the PNA is a naturally

occurring atmospheric phenomenon driven by intrinsic variability of the atmosphere, a La Niña in the tropical Pacific can project onto a negative phase PNA pattern [e.g., Straus and Shukla 2002]. In addition, since the Gulf-to-U.S. moisture transport may be enhanced by a warmer GoM, the sea surface temperature (SST) anomaly in the GoM may also affect U.S. tornado activity. During the decay phase of La Niña in spring, the GoM is typically warmer than usual [Alexander and Scott 2002]. Therefore, the Gulf-to-U.S. moisture transport could be increased during the decay phase of La Niña in spring. Nevertheless, none of these (i.e., PNA, GoM SST, and La Nina) are significantly correlated with the number of intense tornadoes in AM (Table 1).

2.2 *Trans-Niño, a potential predictor of major tornado outbreaks in the U.S.*

Among the long-term climate patterns considered in Table 1, only the Trans-Niño (TNI) is significantly correlated (r = 0.33) with the number of intense U.S. tornadoes in AM. As shown in Figure 1, The TNI is defined as the difference in normalized SST anomalies between the Niño-1+2 (10S° - 0°; 90°W - 80°W) and Niño-4 (5°N - 5°S; 160°E - 150°W) regions and represents the evolution of the ENSO in the months leading up to the event and the subsequent evolution with opposite sign after the event [Trenberth and Stepaniak, 2001]. A recent study showed that the TNI index better represent ENSO phase evolution in spring than the conventional ENSO indices [Lee et al., 2014].

To better understand the potential link between the TNI and U.S. tornado activity, Lee et al. [2013] ranked the years from 1950 to 2010 (61 years in total) based on the number of intense U.S. tornadoes in AM. The top ten years are characterized by an anomalous upper-level cyclone over North America that advects more cold and dry air to the U.S. (Figure 2a), increased Gulf-to-U.S. moisture transport (Figure 2b) and increased lower-level vertical wind shear over the central and eastern U.S. (Figure 2c), whereas the bottom ten years are associated with an anomalous upper-level anticyclone over North America (Figure 2d), decreased Gulf-to-U.S. moisture transport (Figure 2e) and decreased lower-level vertical wind shear over the central and eastern U.S. (Figure 2f).

Table 2. The total of 61 years from 1950 to 2010 are ranked based on the detrended number of intense U.S. tornadoes in AM. The top ten most active U.S. tornado years are listed with ENSO phase in spring and TNI index in AM for each year. Strongly positive (i.e., the upper quartile) and negative (i.e., the lower quartile) TNI index values are in bold and italic, respectively.

Ranking	Year	ENSO phase in spring	TNI index (detrended)
1	1974	La Niña persists	**1.30 (1.48)**
2	1965	La Niña transitions to El Niño	**1.39 (1.54)**
3	1957	La Niña transitions to El Niño	**0.57 (0.69)**
4	1982	El Niño develops	*-1.11* (*-0.89*)
5	1973	El Niño transitions to La Niña	-0.42 (-0.24)
6	1999	La Niña persists	**0.47 (0.75)**
7	1983	El Niño decays	**1.86 (2.08)**
8	2003	El Niño decays	*-1.24* (*-0.94*)
9	2008	La Niña decays	**1.41 (1.73)**
10	1998	El Niño transitions to La Niña	**1.69 (1.97)**

As in the top ten extreme tornado outbreak years, the top ten positive TNI years are also characterized by an anomalous upper-level cyclone over North America (Figure 3a), increased

Gulf-to-U.S. moisture transport (Figure 3b), and increased low-level vertical wind shear values over the east of the Rockies (Figure 3c). Because of these large-scale atmospheric conditions, the number of intense U.S. tornadoes in AM during the top ten positive TNI years is nearly doubled from that during ten neutral TNI years (Figure 4). Consistent with these findings, among the top ten extreme tornado outbreak years, seven years including the top three are identified with a strongly positive phase (i.e., within the upper quartile) TNI as shown in Table 2.

To further explore the potential link between the TNI and the number of intense U.S. tornadoes in AM, Lee et al. [2013] performed a series of AGCM experiments by using version 3.1 of the NCAR community atmospheric model coupled to a slab mixed layer ocean model (CAM3). Model experiments were performed by prescribing various composite evolutions of SSTs in the tropical Pacific region (15°S–15°N; 120°E-coast of the Americas) while predicting the SSTs outside the tropical Pacific using the slab ocean model. Two sets of ensemble runs were performed. In the first experiment (EXP_CLM), the SSTs in the tropical Pacific region are prescribed with climatological SSTs. In the second experiment (EXP_TN1), the composite SSTs of the ten positive phase TNI years are prescribed in the tropical Pacific region. In EXP_TN1 (Figure 5), an anomalous upper-level cyclone is formed over North America that brings more cold and dry air to the U.S., and both the Gulf-to-U.S. moisture transport and the lower-level vertical wind shear over the central and eastern U.S. are increased, all of which are large-scale atmospheric conditions conducive to intense tornado outbreaks over the U.S. Therefore, these model results support the hypothesis that a positive phase of the TNI with cooling in the central tropical Pacific (CP) and warming in the eastern tropical Pacific (EP) enhances the large-scale differential advection in the central and eastern U.S. and increases the low-level vertical wind shear therein, thus providing large-scale atmospheric conditions conducive to intense tornado outbreaks over the U.S.

Further model experiments in Lee et al. [2013] revealed that the warming in the eastern tropical Pacific increases convection locally, but also contributes to suppressing convection in the central tropical Pacific. This in turn works constructively with cooling in the central tropical Pacific to force a strong and persistent negative phase Pacific – North American (PNA)-like teleconnection pattern in spring that increases both the upper-level westerly and lower-level southeasterly flow over the central and eastern U.S. These anomalous winds bring more cold and dry upper-level air from the high-latitudes and more warm and moist lower-level air from the Gulf of Mexico converging into the U.S. east of the Rocky Mountains, while also increasing the low-level vertical wind shear therein. According to this study, a distinctive feature of the 2011 Trans-Niño event is warming in the western tropical Pacific that further aided to suppress convection in the central tropical Pacific and thus contributed to strengthening the teleconnection response in the central and eastern U.S. in favor of increased U.S. tornado activity.

2.3 *Climatic role of North American low-level jet in U.S. regional tornado activity*

Recent studies by Munoz and Enfield [2011] and Weaver et al. [2012] analyzed regional connectivity of North American low-level jets (NALLJ) to springtime tornadic activity. Weaver et al. [2012] extracted preferred modes of NALLJ variability for 1950-2010 and used them to identify three regions over the U.S. based on regional footprints of NALLJ activity. Connectivity of the regional NALLJ modes and tornadic activity to tropical Pacific SST variations indicated that the structure of SST linkages is highly dependent on the selected region and multidecadal epoch. In particular, they found that SST variability patterns similar to the Pacific Decadal Oscillation (PDO) are linked to northern Great Plains tornadoes and NALLJ Mode-1, and the TNI pattern to southeast tornadoes and NALLJ Mode-2. All SST regressions are stronger in the

more recent decades (1979-2010) when compared to the full 1950-2010 time period. The influence of NALLJ variability on the tornadic environment was also assessed and showed interesting regional spatial patterns in anomalies of CAPE, helicity (or vertical wind shear), and the lifted index.

3. Research objectives

Recent tornado outbreaks over the U.S. have caused devastating societal impacts with significant loss of life and property, prompting the need to identify and understand long-term climate signals that may provide seasonal predictability for intense tornado outbreaks over the U.S. A recent study by Lee et al. [2013] used both observations and model experiments to show that an optimal springtime ENSO SST pattern may enhance large-scale atmospheric processes conducive to tornado outbreaks in the U.S. Therefore, the main goal of this proposal is to evaluate seasonal (1 ~ 3 months) prediction skill for springtime ENSO phase evolution and its relation to tornado outbreaks in the U.S. in the North American Multi Model Ensemble Phase 2 (NMME-2) system.

4. Methodology

4.1 *Severe Weather Database* (*SWD*)

The severe weather database (SWD) from the National Oceanic and Atmospheric Administration indicates that the number of total U.S. tornadoes (i.e., from F0 to F5 in the Fujita-Pearson scale) during the most active tornado months of March, April and May (MAM) has been steadily increasing since 1950. However, due to numerous known deficiencies in the SWD, including improvements in tornado detection technology and changes in damage survey procedure over time, one must be cautious in attributing this secular increase in the number of U.S. tornadoes to a specific long-term climate signal [Brooks and Doswell 2001; Verbout et al. 2006]. Since intense and long-lived tornadoes are much more likely to be detected and reported even before a national network of Doppler radar was built in the 1990s, the number of significant (i.e., from F2 to F5 in the Fujita-Pearson scale) and intense (i.e., from F3 to F5 in the Fujita-Pearson scale) U.S. tornadoes in MAM during 1950-2013 obtained from the SWD will be used in this study.

However, it is important to realize that the number of tornadoes may not be the proper metric for representing tornado activity in a given year. For instance, 60 out of the 88 intense U.S. tornadoes in MAM of 1974 occurred on one convective day. Thus, some years with a large number of tornadoes are not qualified as outbreak years if the single day with the largest number of tornadoes in each year is taken out. Due to this limitation in using the number of tornadoes as a tornado metric, it is important that we explore and test different tornado indices. Another metric that we will use is the significant (or intense) U.S. tornado-days, which can be obtained by counting the number of days in which more than a threshold number of significant (or intense) tornadoes occurred [e.g., Verbout et al. 2006]. The threshold number is the upper 25% in the number of significant (intense) U.S. tornadoes in a given day of MAM during 1950-2013 [Lee et al., 2013].

4.2 *North American Multi Model Ensemble Phase 2* (*NMME-2*)

Currently, the NMME-2 models include NOAA/NCEP CFSv2, NASA/GSFC GEOS5, NCAR/UM CCSM4.0, NCAR CESM, NOAA/GFDL CM1, FLORa06, and FLORb01, Environment Canada CanCM3 and CanCM4. These models are global, high-resolution, coupled atmosphere-ocean-land surface-sea ice forecast systems and cover the retrospective forecast

period of 1982-2010. For example, the CFSv2's atmosphere resolution is about 38 km (T382) with 64 levels extending from the surface to 0.26 hPa. The CFSv2 ocean model is 0.25° at the equator, extending to a global 0.5° beyond the tropics, with 40 levels to a depth of 4737m. The CFSv2 land surface model has 4 soil levels and the global sea ice model has 3 levels. The CFSv2 atmospheric model contains observed variations in carbon dioxide (CO_2), together with changes in aerosols and other trace gases and solar variations. With these variable parameters, the analyzed states include estimates of changes in the Earth system climate due to these factors. All available conventional and satellite observations were assimilated in the CFSv2. The CFSv2 covers the period of 1982–2010 with a 24-member ensemble forecast per calendar month out to nine months into the future [Saha et al. 2010].

Kirtman et al. [2014] describe the NMME-2 system, its development and rationale, and show the improved performance of the NMME-1 system over the CFSv2 in predicting ENSO indices and U.S. rainfall variability. One of important tasks in our proposed work is to understand the skill and limitations of the NMME-2 system in predicting key regional parameters for the U.S. tornado outbreaks in MAM (the peak of the tornado season) with 1 to 3 months of lead-time (i.e., January, February, and March initializations).

The NMME-2 retrospective forecast data for the period of 1982-2010 will be provided at the server https://www.earthsystemgrid.org/search.html?Project=NMME. Table 3 and 4 show the daily atmosphere and land fields to be mainly used to derive key regional parameters for U.S. tornado outbreaks (e.g., ENSO indices, the low-level wind shear (surface to 850mb), moisture transport, and CAPE).

Table 3. Daily atmospheric and land surface fields (22) available from the NMME-2 retrospective forecasts

Variable	**Var. Name**	**CF Standard Name**
Surface temperature (SST+land)	Ts	surface_temperature
Mean sea level pressure	Psl	air_pressure_at_sea_level
10m wind (u)	Uas	eastward_wind
10m wind (v)	Vas	northward_wind
10m specific humidity	Qas	Specific humidity

Table 4. Daily atmospheric pressure level fields (5) provided at 850, 500, 200, 100, 50 hPa available from the NMME-2 retrospective forecasts

Variable	**Var. Name**	**CF Standard Name**
Temperature	Ta	air-temperature
Zonal velocity	Ua	eastward_wind
Meridional velocity	Va	northward_wind
Specific humidity	hus	specific_humidity

We are particularly interested in assessing the NMME-2 system prediction skill for the U.S. tornado outbreaks in the MAM of 2011. We are quite confident that we can achieve this because the retrospective forecast period in the NMME-2 models will be soon extended to 2011 and beyond.

4.3 *Proxy tornado indices*

Brooks et al. [2003] used the NCEP-NCAR reanalysis and SWD to examine environmental conditions associated with significant severe thunderstorms and to discriminate between significant tornadic and non-tornadic thunderstorm environments in the central and eastern U.S for the period of 1997-1999. According to this study, significant severe thunderstorms are generated when CAPE ≥ 100 and 2–4 km above ground level lapse rate > 6.5 K km^{-1}, while the so-called tornadic condition requires meeting two additional criteria:

$$2.86\log(S6) + 1.79 \log (CAPE) > 8.36, \quad (1)$$

$$2.74S1 - 2.99\times10^{-4}\ LCL - 3.06\times10^{-4}\ ELV > 1.93, \quad (2)$$

where S6 is the 0 – 6 km wind shear, S1 is the 0 – 1 km wind shear, LCL is the mean layer lifted condensation level (in m), and ELV is the station elevation (in m).

In this proposed work, we will use a similar but much-simplified approach using only the seasonally averaged variables derived from the NMME-2 analysis (i.e., 0 ~ 24-hour forecast) and SWD. Our strategy here is to perform a partial regression analysis of key variables with respect to tornado indices. Linear partial regression, which is used in the context of multiple linear regression analysis, is an effective tool to model (or predict) one dependent variable (or predictand) using multiple independent variables (or predictors) when the independent variables are not orthogonal to each other. The basic concept is quite similar to that of partial correlation. It basically gives the amount of increase in the dependent variable with respect to the unit increase in one independent variable while all other independent variable are held constant.

To construct the partial regression model, we will first attempt with five predictors. Two ENSO indices that best represent the springtime ENSO phase evolution, namely the TNI and El Niño Modoki (EMI) indices, will be used [Lee et al., 2014]. We will also use the low-level wind shear (surface to 850mb), moisture transport, and CAPE averaged over the central and eastern U.S. region frequently affected by intense tornadoes (30º–40ºN, 100º–80ºW) [Lee et al. 2013].

Figure 6 shows the number of significant U.S. tornadoes in MAM versus the proxy index derived from the linear partial regression model, which is constructed based on the five predictors (i.e., TNI and EMI indices, and low-level wind shear, moisture transport and CAPE averaged over the central and eastern U.S. region) obtained from the 20th century reanalysis [20CR Compo et al., 2011]. The two time series are significantly and highly correlated (r = 0.72) clearly suggesting that the linear partial regression model is a valuable tool.

The proxy index will be regenerated based on the NCEP-NCAR reanalysis [Kalney et al., 1996] to explore if the correlation is robust. The proxy index for the period of 1982 - 2010 will be also updated using the NMME-2 analysis. If necessary, a simple linear bias correction will be applied to the 20CR-based (or NCEP reanalysis-based) proxy index to minimize the systematic difference between the 20CR (or NCEP reanalysis) and the NMME-2 analysis.

4.4 *Probability of U.S. tornado outbreak*

It should be note that the proxy index derived from the partial regression model is not an accurate measure of the number of significant tornadoes (i.e., large RMSE) as shown in Figure 6. For instance, in the MAM of 2011, 135 significant tornadoes occurred in the U.S. However, the partial regression model predicts only 71. This means that it is not practical to predict the number of significant tornadoes for a given year. Therefore, as a more practical alternative, we propose a new metric, “probability of U.S. tornado outbreak”.

This new metric provides the probability that the number of significant U.S. tornadoes for a given year exceeds a threshold value. To compute this metric, we first need to define "outbreak" when the number of significant tornadoes in MAM exceed a threshold value. Then, the number of years during which the proxy index exceeds the threshold value can be counted. For example, if we select the lowest of the upper tercile as the threshold value, which is 104 in this case, there are 19 years during which the proxy index exceeds 104. Out of the 19 years, the actual number of significant tornadoes exceeded 104 in 12 years, yielding 75% chance of tornado outbreak. What this means is that if the proxy index exceeds 104, we have about 75% chance to have an outbreak. Similarly, if the proxy index is in between 64 (the highest of the lower tercile) and 104, we have about 31% of chance of having an outbreak. Therefore, as summarized in Figure 6b, the probability of U.S. tornado outbreak for a given year ranges between 0 and 75%.

5. Proposed tasks

Our work will be comprised of three tasks: (task-1) evaluate the NMME-2 prediction skill for springtime ENSO phase evolution and its relation to U.S. tornadic environments; (task-2) construct proxy tornado indices using the NMME-2 analysis; (task-3) analyze the NMME-2 prediction skill for the occurrence of U.S. tornado outbreaks.

Task-1) Evaluate the NMME-2 prediction skill for springtime ENSO phase evolution and its relation to U.S. tornadic environments

Every ENSO event is somewhat different from others. This is especially true during the springtime ENSO phase evolution. For example, during the decay phase, the SST anomalies in eastern tropical Pacific often switch to the opposite sign (e.g., 2007-2008 La Niña). In some cases, the SST anomalies in the central and eastern tropical Pacific dissipate together during or after spring (e.g., 1991-1992 El Niño), or further evolve into the onset of another ENSO event with either the same or opposite sign in the subsequent months (e.g., 1986-1987 El Niño). In rare cases, the SST anomalies in the eastern tropical Pacific persist much longer than those in the central tropical Pacific, as reported for the decay of the two extreme El Niños in 1982-1983 and 1997-1998. As such, forecasting ENSO is considerably more difficult for boreal spring than other seasons.

Lee et al. [2013] showed that the seasonal predictability of U.S. tornado outbreaks, if there is any, could originate from springtime ENSO phase evolution and its atmospheric bridge to the U.S. Therefore, our first task is to evaluate seasonal (1 ~ 3 months) prediction skill for springtime ENSO phase evolution and its relation to U.S. tornadic environments (i.e., low-level vertical wind shear, moisture transport and CAPE over the continental U.S.) in the NMME-2 system. The skill of NMME-2 system for predicting various ENSO indices, particularly the TNI and EMI indices, and their relations to U.S. tornadic environments will be assessed targeting MAM. To assess the seasonal forecasting skill of NMME-2 system, anomaly correlations between the NMME-2 analysis and the lead-time dependent forecasts (and other evaluation metrics such as RMSE and bias) will be applied to the five variables, namely the TNI and EMI indices, and the low-level vertical wind shear, moisture transport and CAPE averaged over the central and eastern U.S. region (30º–40ºN, 100º–80ºW).

Task-2) Construct proxy tornado indices using the NMME-2 analysis

As summarized in section 4.3, we will use the seasonally averaged variables derived from the NMME-2 analysis (i.e., 0 ~ 24-hour forecast) and SWD to perform a partial regression analysis

with respect to tornado indices. To construct the partial regression model, we will first attempt with five predictors, namely the TNI and EMI indices, and low-level wind shear, moisture transport and CAPE averaged over the central and eastern U.S. region frequently affected by intense tornadoes (30º–40ºN, 100º–80ºW). For the periods not covered by the NMME-2 (i.e., 1950-1981 and 2011-present), the five predictors will be obtained from the 20CR (or NCEP-NCAR reanalysis). If necessary, a simple linear bias correction will be applied to the 20CR-based (or NCEP-NCAR reanalysis-based) proxy index to minimize the systematic difference between the 20CR (or NCEP-NCAR reanalysis) and the NMME-2 analysis.

We will also consider other variables. For example, synoptic activity, which can be represented as variance of 5-day high-pass filtered meridional winds at 300 hPa, will be tested if it adds value to the partial regression model.

Task-3) Analyze the NMME-2 prediction skill for the occurrence of U.S. tornado outbreaks

Our next task is to evaluate the seasonal (1 ~ 3 months) prediction skill of the NMME-2 system for the observed tornado indices targeting MAM. First, we will construct lead-time dependent proxy tornado index based on the five predictors. Then, we will use various evaluation metrics, namely anomaly correlation, RMSE, mean absolute error, amplitude and biases to assess the NMME-2 skill and lead-time dependence in forecasting the observed tornado indices.

For example, the CFSv2 includes a 4-member ensemble initialized every 5th day of each year for 1982-2010 beginning on January 1st. The lead-dependent proxy tornado index for MAM will be constructed from the monthly output of all reforecasts initialized between January 1 and April 1 for 1982-2010, comprising the total of 76 ensemble members. Then, we can compute the anomaly correlation (and other evaluation metrics) between the observed MAM tornado index and the proxy MAM tornado index derived from the 28-member ensemble forecasts initialized between January 1 and January 30 to measure the prediction skill of the CFSv2 with three-month lead-time, and etc. A similar procedure will be applied for the other NMME-2 models to assess the skill of individual models and for the NMME-2 system.

6. Future tasks

Completing the above three tasks, we will learn if the NMME-2 has a useful skill to forecast U.S. tornado activity in MAM. If it does, we would like to explore an experimental seasonal outlook for U.S. tornado outbreaks. However, it is unlikely that we can complete beyond the first three tasks within one-year period. Therefore, the following two tasks are saved for future funding opportunity.

Task-4) Explore an experimental seasonal outlook for U.S. tornado outbreaks

If the NMME-2 has a useful skill to forecast U.S. tornado activity in MAM, the next task is to explore an experimental seasonal outlook for U.S. tornado outbreaks. The experimental outlook product will provide the probability of U.S tornado outbreaks, which will be computed based on the methodology described in section 4.4. Using the NMME-2 system forecasts, the probability of the U.S. tornado outbreaks for a given year can be estimated using the following equation:

$$\text{Prob. (\%)} = (M_1 \times P_1 + M_2 \times P_2 + M_3 \times P_3) \times N^{-1}, \quad (3)$$

where N is the total number of the NMME-2 ensemble forecasts, M_1 is the number of ensemble members with their MAM proxy tornado indices exceeding the threshold value for outbreak, M_2 is the number of ensemble members with their MAM proxy tornado indices fall between the threshold value for outbreak and the upper limit value for low-activity, M_3 is the number of ensemble members with their MAM proxy tornado indices below the upper limit value for low-activity. P_1, P_2, and P_3 are the probability of outbreaks, which will be determined from the NMME-2 analysis, 20CR and SWD as described in section 4.4.

For example, if the threshold number of significant tornadoes for outbreak is 104, the upper limit number of significant tornadoes for low-activity is 64, P_1 = 75%, P_2 = 31%, P_3 = 0% (these values will be later updated using the NMME-2 analysis), M_1 = 67, M_2 = 28, and M_3=5, the probability of U.S. tornado outbreak is 59% (= [67×75 + 28×31 + 5×0] × 100^{-1}). As shown in Table 3, depending on probability of U.S. tornado outbreaks obtained from the NMME-2 system, four-stage alert levels, i.e., Low (Green), Moderate (Yellow), High (Red), and Extreme (Black), may be issued in January 1, February 1 and March 1.

To measure the accuracy of the probabilistic U.S. tornado outbreak prediction, we will use various evaluation merics, including Brier skill score:

$$BS = \frac{1}{N}\sum_{i=1}^{N}(P_i - O_i)^2 , \qquad (4)$$

where P is the forecasted probability (0 ~ 1), O is the actual outcome of the event (1 if an outbreak occurs, and 0 if an outbreak does not occur) and N is the number of forecasting instances.

Table 3. An example of seasonal outlook for U.S. tornado outbreaks. Depending on probability of U.S. tornado outbreaks obtained from the NMME-2 system, four-stage alert levels, i.e., Low (Green), Moderate (Yellow), High (Red), and Extreme (Black), may be issued in January 1, February 1 and March 1.

Probability of U.S. tornado outbreaks in MAM	Alert Level	Description
Above 60%	Extreme	Highly enhanced chance of outbreak
40 – 60%	High	Enhanced chance of outbreak
20 – 40%	Moderate	Normal chance of outbreak
Below 20%	Low	Below normal chance of outbreak

Task-5) Explore an experimental seasonal outlook for *regional* U.S. tornado outbreaks

It is important to point out that tornado outbreaks in the U.S. occur in regional scale. In the MAM of 2011, for instance, the majority of the significant tornadoes occurred in the Southeast. Therefore, in the next task, we would like to explore if the seasonal outlook described in the task-4 can be achieved in regional scale. The main steps to compute the probability of regional U.S. tornado outbreaks are identical to those described in task-2, -3 and -4, except that the observed and proxy tornado indices are constructed separately for predefined regions. For instance, we can use three U.S. regions, namely, the South, Central and Southeast as defined by the National Climate Data Center.

We can also divide the U.S. into 5º×5º boxes. Figure 7 shows the number of significant U.S. tornadoes in MAM versus the proxy index for the region of 35ºN-40ºN and 90ºW-95ºW. Figure

8 is the same as Figure 7 expect for the region of 30ºN-35ºN and 85ºW-90ºW. As expected, the two regions have very different time series in the observed number of significant tornadoes. The observed and proxy time series are significantly and highly correlated in both regions (r = 0.52 ~ 0.56) suggesting that it may be possible to issue a seasonal outlook for *regional* U.S. tornado outbreaks.

7. Work plan and collaboration with S. Weaver (CPC)

S.-K. Lee will primarily carry out all of the three proposed tasks, while R. Atlas, C. Wang will help and guide S.-K. Lee. S. Weaver is a collaborator of this proposed work. Currently, he is a research meteorologist in the operational monitoring & operational prediction branches of the NOAA Climate Prediction Center (CPC) in College Park, Maryland. If this proposal is funded, we will collaborate with S. Weaver in our efforts to analyze the NMME-2 prediction skill for the occurrence of U.S. tornado outbreaks (task-3). His expertise on the variability of the North American low-level jet and its relation with U.S. tornado activity will be essential for successfully completing the proposed works.

References

Alexander, M. A. and J. D. Scott (2002), The influence of ENSO on air-sea interaction in the Atlantic. *Geophys. Res. Lett.*, **29**, doi:10.1029/2001GL014347.

Brooks, H. E., C. A. Doswell III (2001), Some aspects of the international climatology of tornadoes by damage classification, *Atmos. Res*., **56**, 191– 201.

Brooks, H. E., J. W. Lee, and J. P. Cravenc (2003), The spatial distribution of severe thunderstorm and tornado environments from global reanalysis data, *Atmos. Res*., **67-68**, 73-94.

Compo, G. P., et al. (2011), The twentieth century reanalysis project, *Q. J. R. Meteorol. Soc.*, 137, 1–28, doi:10.1002/qj.776.

Cook, A. R., and J. T. Schaefer (2008), The relation of El Niño–Southern Oscillation (ENSO) to winter tornado outbreaks, *Mon. Wea. Rev*., **136**, 3121–3137.

Ding, Q., and coauthors (2011), Tropical-extratropical teleconnections in boreal summer: Observed interannual variability. *J. Climate*, **24,** 1878-1896.

Doswell, C. A. III, and L. F. Bosart (2001), Extratropical synoptic-scale processes and severe convection. Severe Convection Storms, *Meteor. Monogr*., **28**, Amer. Meteor. Soc., 27-69.

Doswell, C. A. III, H. E. Brooks, and N. Dotzek (2009) On the implementation of the Enhanced Fujita Scale in the USA. *Atmos. Res*., **93**, 554-563, doi:10.1016/j.atmosres.2008.11.003.

Hoerling, M. P., and A. Kumar (1997), Why do North American climate anomalies differ from one El Niño event to another?, *Geophys. Res. Lett*., **24**, 1059-1062.

Kalnay, E., and Coauthors, 1996: The NCEP/NCAR 40-Year Reanalysis Project. *Bull. Amer. Meteor. Soc*., **77**, 437–471.

Kirtman, B. P. and coauthors (2014), The North American Multimodel Ensemble: Phase-1 Seasonal-to-Interannual Prediction; Phase-2 toward Developing Intraseasonal Prediction. Bull. Amer. Meteor. Soc., 95, 585–601. doi: http://dx.doi.org/10.1175/BAMS-D-12-00050.1.

Kumar, A., and M. P. Hoerling (2003), The nature and causes for the delayed atmospheric response to El Niño. *J. Climate*, **16**, 1391-1403.

Lee, S.-K., R. Atlas, D. B. Enfield, C. Wang and H. Liu, 2013: Is there an optimal ENSO pattern that enhances large-scale atmospheric processes conducive to major tornado outbreaks in the U.S.? J. Climate, 26, 1626-1642. doi:http://dx.doi.org/10.1175/JCLI-D-12-00128.1.

Lee, S.-K., B. E. Mapes, C. Wang, D. B. Enfield and S. J. Weaver, 2014: Springtime ENSO phase evolution and its relation to rainfall in the continental U.S. Geophys. Res. Lett., 41, 1673-1680. doi:10.1002/2013GL059137.

Marzaban, C., and J. T. Schaefer (2001), The correlation between U.S. tornadoes and Pacific sea surface temperatures. *Mon. Wea. Rev.*, **129**, 884-895.

Munoz, E., and D. B. Enfield (2010), The boreal spring variability of the Intra-Americas low-level jet and its relation with precipitation and tornadoes in the eastern United States, *Clim. Dyn*. **36**, 247–259.

Ropelewski, C. F., and M. S. Halpert (1987), North American precipitation and temperature patterns associated with El Niño/Southern Oscillation (ENSO). Mon. Wea. Rev., 114, 2352-2362.

Saha, S., and coauthors (2010), The NCEP Climate Forecast System Reanalysis. *Bull. Amer. Meteor. Soc*., **90**, 1015-1057.

Straus, D. M., and J. Shukla (2002), Does ENSO force the PNA?, *J. Climate.*, **15**, 2340–2358.

Trenberth, K. E., and D. P. Stepaniak (2001), Indices of El Niño evolution, *J. Clim.*, **14**, 1697–1701.

Verbout, S. M., H. E. Brooks, L. M. Leslie, and D. M. Schultz (2006), Evolution of the U.S. tornado database: 1954-2003. *Wea. Forecasting*, **21**, 86-93.

Weaver, S. J., S. Baxter, and A. Kumar (2012), Climatic role of North American low-level jets on U.S. regional tornado activity. *J. Clim.*, **25**, 6666–6683.

Whitney Jr., L. F., and J. E. Miller (1956), Destabilization by differential advection in the tornado situation 8 June 1953. *Bull. Amer. Meteor. Soc*., **37**, 224–229.

Whiton, R. C., P. L. Smith, S. G. Bigler, K. E. Wilk, A. C. Harbuck (1998a), History of operational use of weather radar by U.S. Weather Services. Part I: The Pre-NEXRAD Era. *Wea. Forecasting*, **13**, 219–243.

Whiton, R. C., P. L. Smith, S. G. Bigler, K. E. Wilk, A. C. Harbuck (1998b), History of operational use of weather radar by U.S. Weather Services. Part II: Development of operational doppler weather radars. *Wea. Forecasting*, **13**, 244–252.

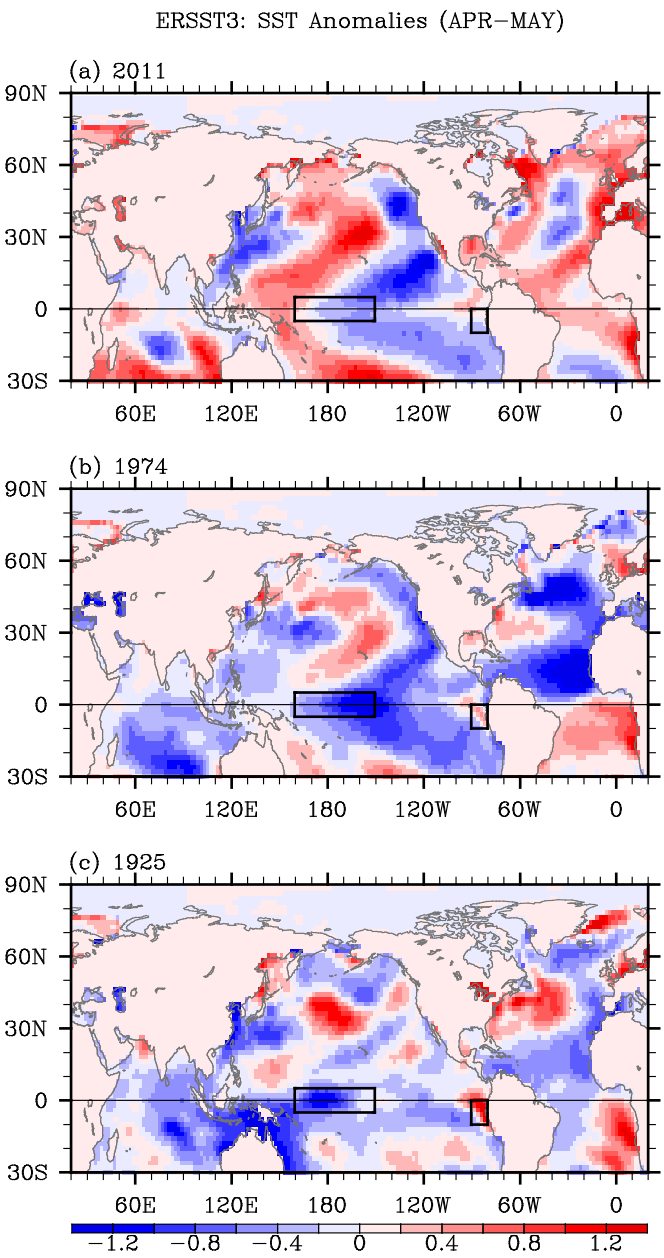

Figure 1. Anomalous SSTs in AM of three historical U.S. tornado outbreak years, namely (a) 2011, (b) 1974 and (c) 1925, obtained from ERSST3. The unit is °C.

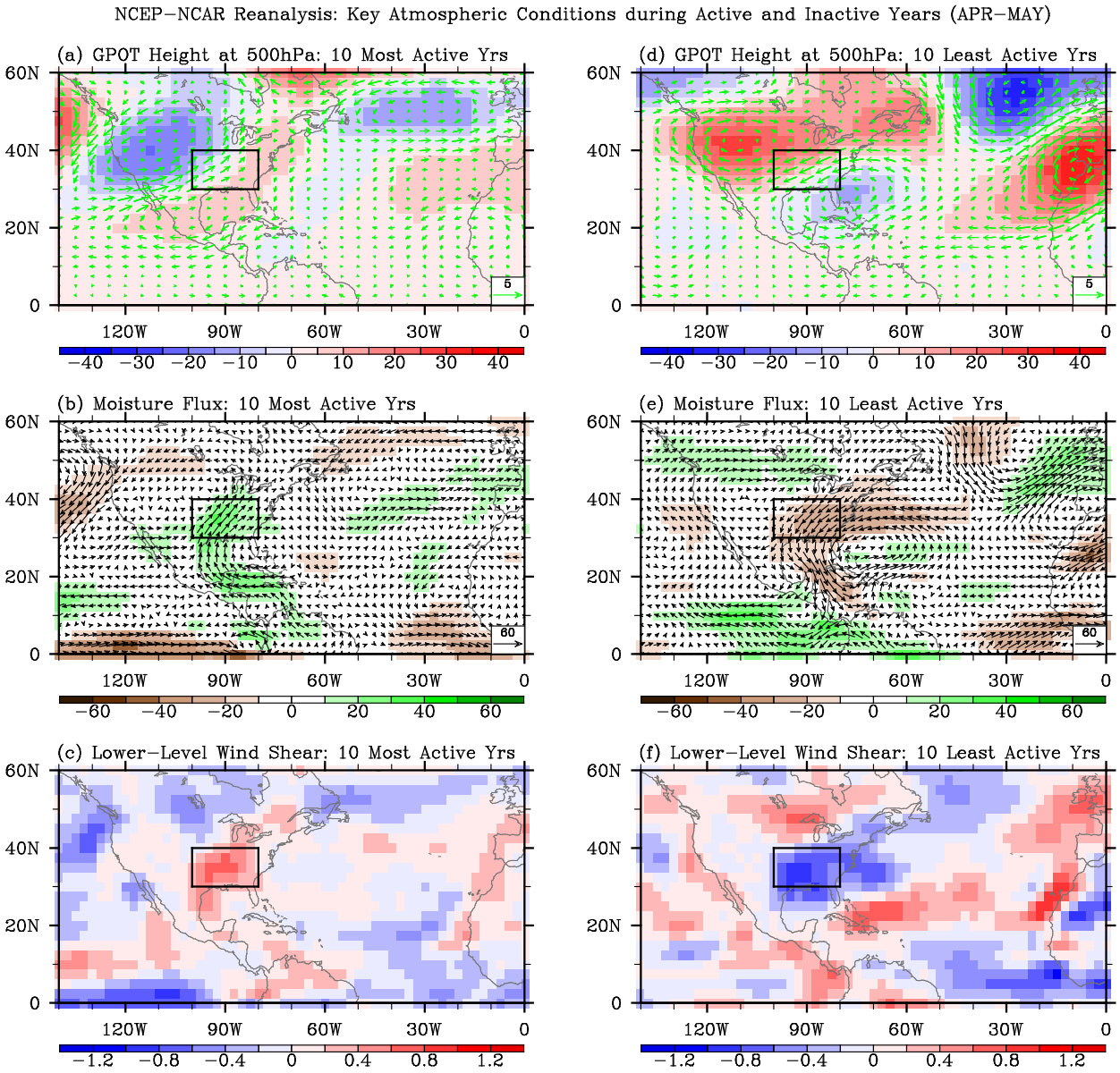

Figure 2. Anomalous geopotential height and wind at 500 hPa, moisture transport and lower-level (850 – 1000 hPa) vertical wind shear for the ten most active U.S. tornado years (a, b and c) and the ten least active U.S. tornado years (d, e and f) in AM during 1950-2010 obtained from NCEP-NCAR reanalysis. The units are kg $m^{-1}sec^{-1}$ for moisture transport, m for geopotential height, and m s^{-1} for wind and wind shear. The small box in (a) - (f) indicates the central and eastern U.S. region frequently affected by intense tornadoes (30^{o}N-40^{o}N, and 100^{o}W-80^{o}W). The values of the 90% confidence interval averaged over the box region are 15 (17) and 0.5 (0.4) for b (e) and c (f), respectively.

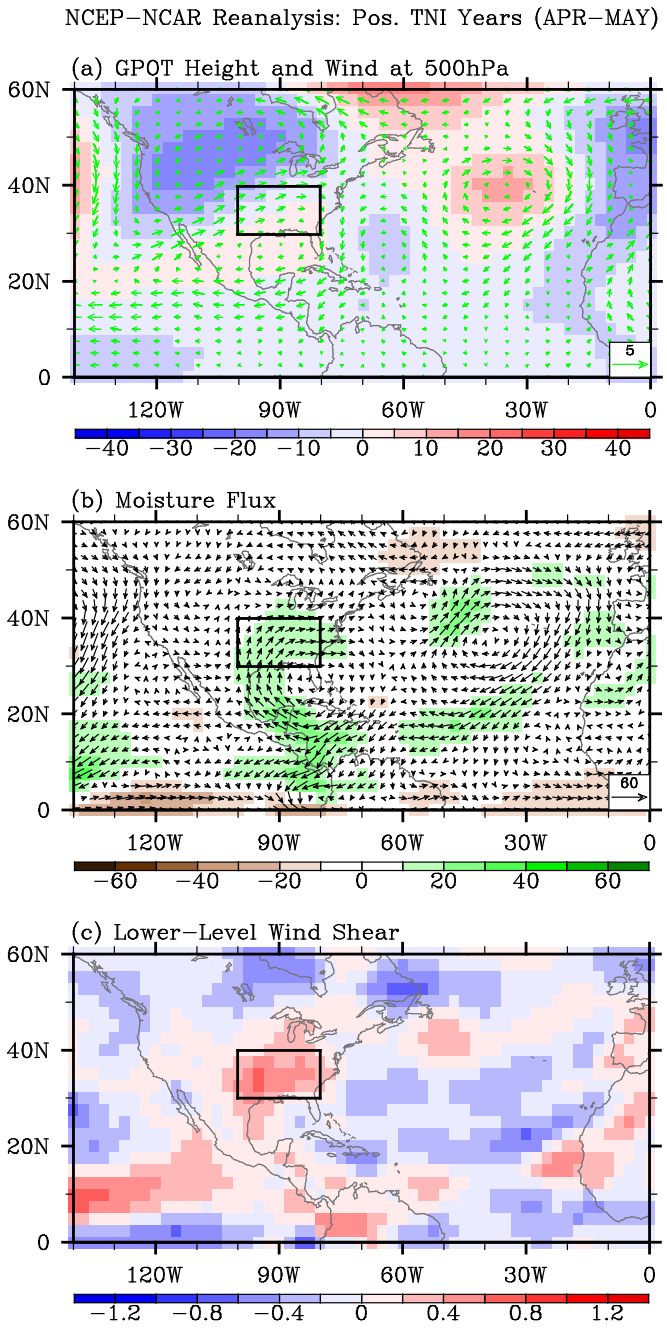

Figure 3. Anomalous (a) geopotential height and wind at 500 hPa, (b) moisture transport and (c) lower-tropospheric (850 – 1000 hPa) vertical wind shear for the top ten positive TNI years in AM during 1950-2010 obtained from NCEP-NCAR reanalysis. The units are kg $m^{-1}sec^{-1}$ for moisture transport, m for geopotential height, and m s^{-1} for wind and wind shear. The small box in (a) - (c) indicates the central and eastern U.S. region frequently affected by intense tornadoes (30^oN-40^oN, and 100^oW-80^oW). The values of the 90% confidence interval averaged over the box region are 16 and 0.5 for b and c, respectively.

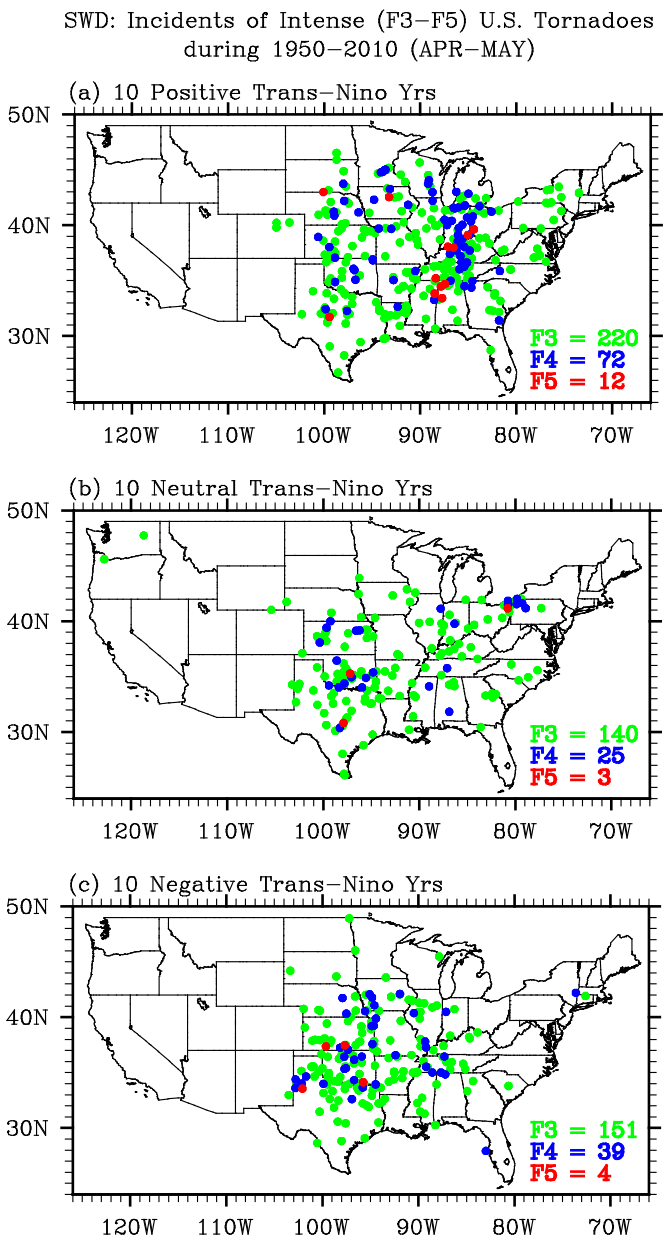

Figure 4. Incidents of intense (F3-F5) U.S. tornadoes in AM for (a) the top ten positive TNI year, (b) ten neutral TNI years, and (c) the top ten negative TNI years during 1950-2010 obtained from SWD. Green color is for F3, blue color for F4 and red color for F5 tornadoes.

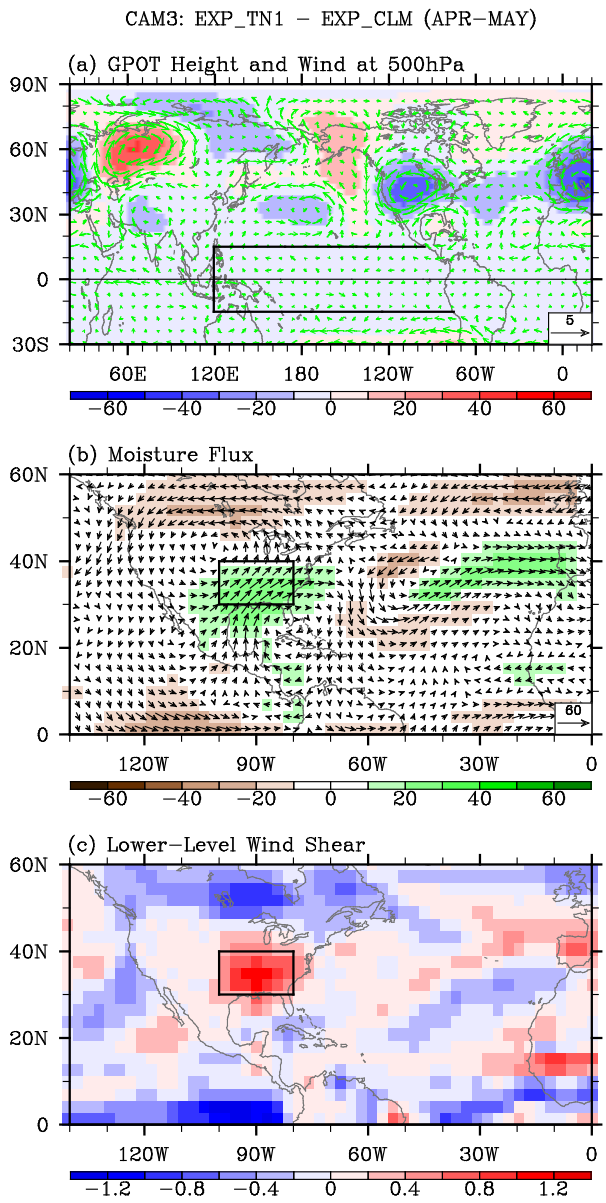

Figure 5. Simulated anomalous (a) geopotential height and wind at 500 hPa, (b) moisture transport and (c) lower-level (850 – 1000 hPa) vertical wind shear in AM obtained from EXP_TN1 – EXP_CLM. The units are kg m^{-1} sec^{-1} for moisture transport, m for geopotential height, and m s^{-1} for wind and wind shear. Thick black lines in (a) indicate the tropical Pacific region where the model SSTs are prescribed. The small box in (b) and (c) indicates the central and eastern U.S. region frequently affected by intense tornadoes (30°N-40°N, and 100°W-80°W). The values of the 90% confidence interval averaged over the box region are 17 and 0.5 for b and c, respectively.

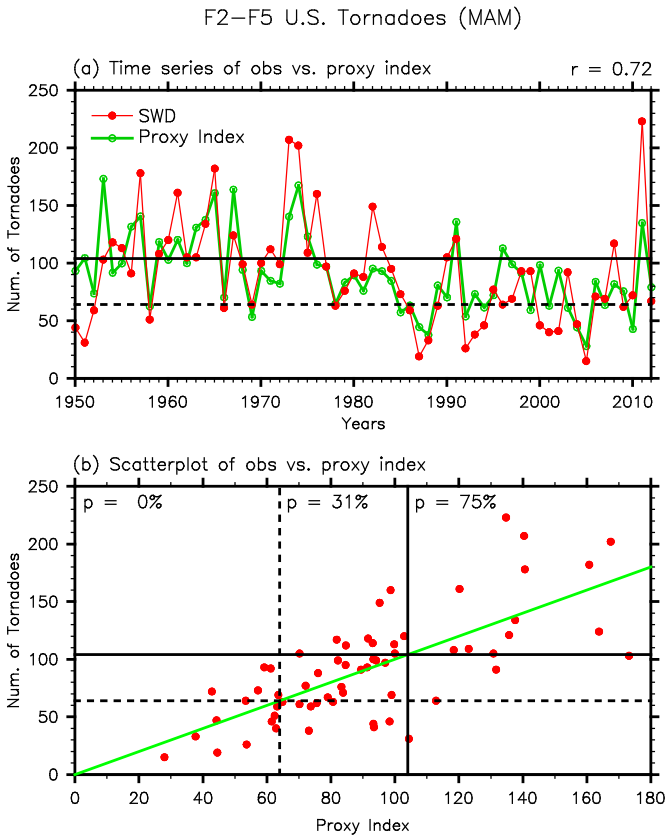

Figure 6. (a) Time series of the number of significant (F2-F5) U.S. tornadoes in MAM versus the proxy index derived from the linear partial regression model, which is constructed based on the five predictors (i.e., TNI and EMI indices, and low-level wind shear, moisture transport and CAPE averaged over the central and eastern U.S. region) obtained from the 20th century reanalysis. (b) Scatterplot of the observed versus proxy number of significant (F2-F5) U.S. tornadoes in MAM. The green line in (b) is the linear regression line, which is above the 99% significance level. The black solid line in (b) indicates the lowest of the upper tercile (104), whereas the black dashed line indicates the highest of the lower tercile (64). The probability of U.S. tornado outbreaks is 75% if the proxy index is above 104, 31% if the proxy index is in between 104 and 64, and 0% if the proxy index is below 64.

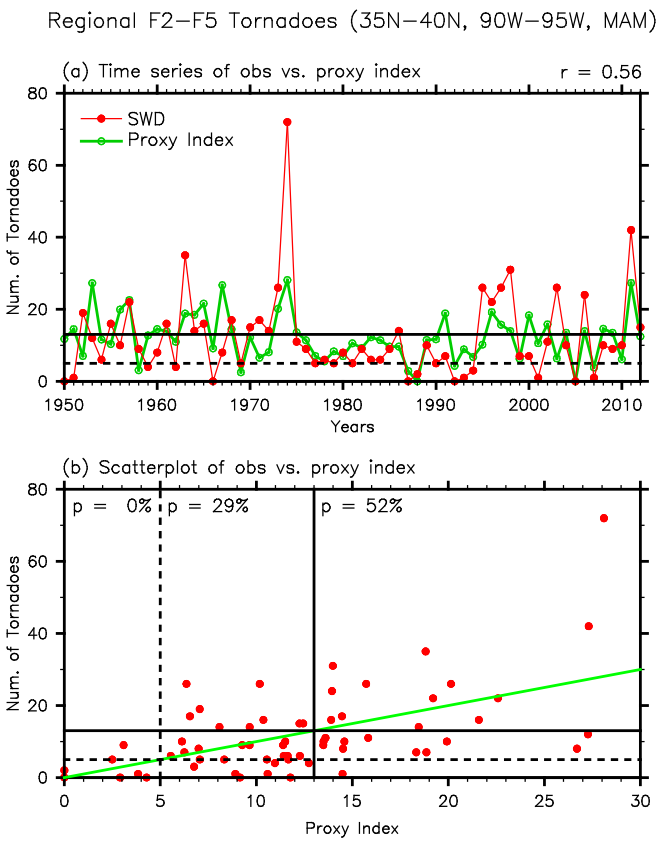

Figure 7. Same as Figure 6 expect that the observed and proxy tornado indices are obtained for the region of 35ºN-40ºN and 90ºW-95ºW.

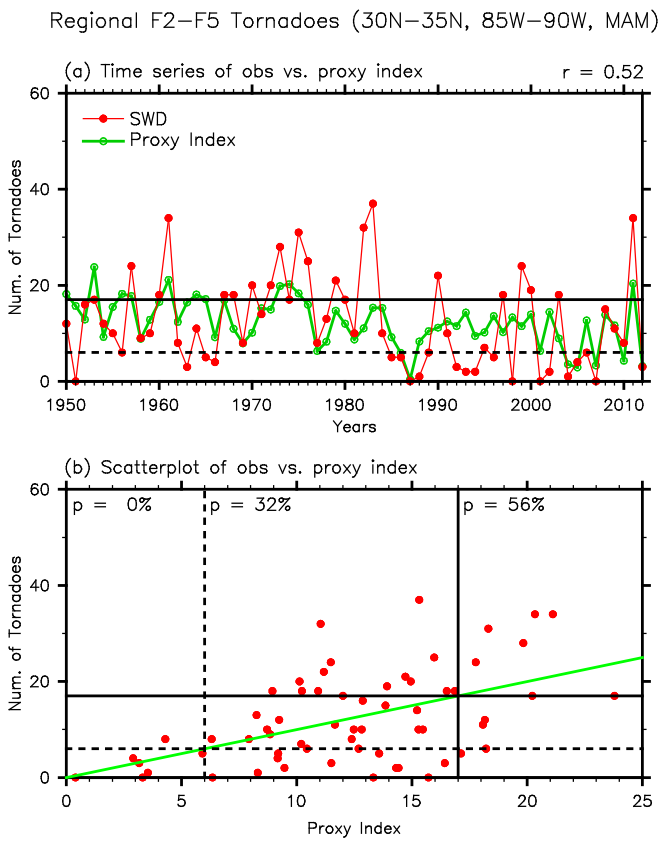

Figure 8. Same as Figure 6 expect that the observed and proxy tornado indices are obtained for the region of 30ºN-35ºN and 85ºW-90ºW.

Budget Justification

Salary requests from NOAA/CPO include funds for S.-K. Lee (4 months) and for a research supporting staff (0.3 months). R. Atlas, and C. Wang will work on this project for one month per year at no salary cost to the project. One trip for attending a scientific meeting for dissemination of scientific results or for collaborating with S. Weaver (NOAA/CPC) is budgeted. Publication page charges are also budgeted.

Salaries			Year 1		Total
Sang-Ki Lee	Lead-PI	4mo	$33,517	4mo	$33,517
Research Associate	Supporting Staff	0.3mo	$1,015	0.3mo	$ 1,015
Fringe Benefits			$13,168		$13,168
Total Salaries & Fringe Benefits			$47,700		$47,700
Domestic Travel (1 trip)			$1,500		$1,500
Air Fare			$600		$600
Per Diem			$300		$300
Lodging			$500		$500
Transportation			$100		$100
Publications			$500		$500
Modified Total Direct Costs			$49,700		$49,700
Indirect Costs 40.0%			$19,880		$19,880
Total Project Costs			**$69,580**		**$69,580**

Curriculum Vitae: Sang-Ki Lee

Cooperative Institute for Marine and Atmospheric Studies, University of Miami
4600 Rickenbacker Causeway, Miami, FL 33149
Sang-Ki.Lee@noaa.gov
http://www.aoml.noaa.gov/phod/people/sklee.html

Education:

PhD, Old Dominion University, Norfolk, Va (Oceanography)	1995
MSc, Old Dominion University, Norfolk, Va (Oceanography)	1993
BSc, Inha University, Incheon, South Korea (Oceanography)	1991

Professional Service:

Scientist, CIMAS, University of Miami	2011 - Present
Associate Scientist, CIMAS, University of Miami	2007 - 2010
Assistant Scientist, CIMAS, University of Miami	2005 - 2007
Postdoctoral Associate, CIMAS, University of Miami	2002 - 2004
Associate Scientist: Maritime Research Institute, Samsung Heavy Industries	1996 - 2001
Graduate Research Assistant, Old Dominion University	1991 - 1995

Refereed publications (last three years):

Cheon, W. G., Y.-G. Park, J. R. Toggweiler, and S.-K. Lee, 2014: The relationship of Weddell polynya and open-ocean deep convection to the Southern Hemisphere westerlies. *J. Phys. Oceanogr*., 44, 694-713. doi: http://dx.doi.org/10.1175/JPO-D-13-0112.1

Ji, X., J. D. Neelin, S.-K. Lee and C. R. Mechoso, 2014: Interhemispheric teleconnections from tropical heat sources in intermediate and simple models. *J. Climate*, 27, 684-697. doi: http://dx.doi.org/10.1175/JCLI-D-13-00017.1.

Lee, S.-K., B. E. Mapes, C. Wang, D. B. Enfield and S. J. Weaver, 2014: Springtime ENSO phase evolution and its relation to rainfall in the continental U.S. *Geophys. Res. Lett*., 41, 1673-1680. doi:10.1002/2013GL059137.

Liu, H., C. Wang, S.-K Lee and D. B. Enfield, 2014: Inhomogeneous influence of the Atlantic warm pool on United States precipitation. *Atmos. Sci. Lett*., doi:10.1002/asl2.521.

Wang, C., L. Zhang, S.-K. Lee, L. Wu and C. R. Mechoso, 2014: A global perspective on CMIP5 climate model biases. *Nature Clim. Change*, 4, 201-205. doi:10.1038/nclimate2118.

Zhang, L., C. Wang and S.-K. Lee, 2014: Potential role of Atlantic warm pool-induced freshwater forcing in the Atlantic meridional overturning circulation: Ocean-sea ice coupled model simulations. *Climate Dynam*., 43, 553-574. doi:10.1007/s00382-013-2034-z.

Lee, S.-K., C. R. Mechoso, C. Wang and J. D. Neelin, 2013: Interhemispheric influence of the northern summer monsoons on the southern subtropical anticyclones. *J. Climate*, 26, 10193-10204. doi:http://dx.doi.org/10.1175/JCLI-D-13-00106.1.

Lee, S.-K., R. Atlas, D. B. Enfield, C. Wang and H. Liu, 2013: Is there an optimal ENSO pattern that enhances large-scale atmospheric processes conducive to major tornado outbreaks in the U.S.? *J. Climate*, 26, 1626-1642. doi:http://dx.doi.org/10.1175/JCLI-D-12-00128.1.

Liu, H., C. Wang, S.-K. Lee and D. B. Enfield, 2013: Atlantic warm pool variability in the CMIP5 simulations. *J. Climate*, 26, 5315-5336, doi: http://dx.doi.org/10.1175/JCLI-D-12-00556.1.

Menary M. B, C. D. Roberts, M. D. Palmer, P. R. Halloran, L. Jackson, R. A. Wood, W. A. Mueller, D. Matei and S.-K. Lee, 2013: Mechanisms of aerosol-forced AMOC variability in a state of the art climate model. *J. Geophys. Res*., 118, 2087-2096, doi:10.1002/jgrc.20178.

Wang, C., L. Zhang, S.-K. Lee, 2013: Response of freshwater and sea surface salinity to variability of the Atlantic warm pool. *J. Climate*, 26, 1249-1267, doi:10.1175/JCLI-D-12-00284.1.

DiNezio, P. N., B. P. Kirtman, A. C. Clement, S.-K. Lee, G. A. Vecchi and A. Wittenberg, 2012: Mean climate controls on the simulated response of ENSO to increasing greenhouse gases. *J. Climate*, 25, 7399-7420, doi: http://dx.doi.org/10.1175/JCLI-D-11-00494.1.

Larson, S., S.-K. Lee, C. Wang, E.-S. Chung, and D. Enfield, 2012. Impacts of non-canonical El Nino patterns on Atlantic hurricane activity. *Geophys. Res. Lett*., 39, L14706, doi:10.1029/2012GL052595.

Liu, H., C. Wang, S.-K. Lee and D. B. Enfield, 2012. Atlantic warm pool variability in the IPCC twentieth-century climate simulations. *J. Climate*, 25, 5612-5628, doi:10.1175/JCLI-D-11-00376.1.

Liu Y., S.-K. Lee, B. A. Muhling, J. T. Lamkin and D. B. Enfield, 2012. Significant reduction of the Loop Current in the 21st century and its impact on the Gulf of Mexico. *J. Geophys. Res*, 117, C05039, doi:10.1029/2011JC007555.

Wang, C., S. Dong, A. T. Evan, G. R. Foltz, and S.-K. Lee, 2012. Multidecadal co-variability of North Atlantic sea surface temperature, African dust, Sahel rainfall and Atlantic hurricanes. *J. Climate*, 25, 5404-5415, doi:10.1175/JCLI-D-11-00413.1.

Five other publications:

Lee S.-K., W. Park, E. van Sebille, M. O. Baringer, C. Wang, D. B. Enfield, S. Yeager, and B. P. Kirtman, 2011. What caused the significant increase in Atlantic Ocean heat content since the mid-20th century? *Geophys. Res. Lett.*, doi:10.1029/2011GL048856.

Lee, S.-K., D. B. Enfield and C. Wang, 2011. Future impact of differential inter-basin ocean warming on Atlantic hurricanes. *J. Climate*, 24, 1264-1275.

Lee, S.-K., C. Wang and D. B. Enfield, 2010: On the impact of central Pacific warming events on Atlantic tropical storm activity. *Geophys. Res. Lett*., 37, L17702, doi:10.1029/2010GL044459.

Lee, S.-K. and C. Wang, 2010: Delayed advective oscillation of the Atlantic thermohaline circulation. *J. Climate*, 23, 1254-1261.

Lee, S.-K., C. Wang and B. E. Mapes, 2009: A simple atmospheric model of the local and teleconnection responses to tropical heating anomalies. *J. Climate*, 22, 272-284.

Curriculum Vitae: Robert M. Atlas

NOAA Atlantic Oceanographic and Meteorological Laboratory
4301 Rickenbacker Causeway, Miami, FL 33149
Robert.Atlas@noaa.gov

Education:

Ph.D. New York University (Meteorology and Oceanography)	1976
M.S. New York University, Meteorology	1973
B.S. Parks College of Aeronautical Technology of St. Louis University, Aeronautics	1970

Professional Service:

Director, Atlantic Oceanographic and Meteorological Laboratory	2005 - Present
Chief Meteorologist, Laboratory for Atmospheres, NASA Goddard Space Flight Center	2003 - 2005
Director, NASA Data Assimilation Office	1998 - 2003
Research Scientist, NASA/Goddard Space Flight Center and Adjunct Professor, University of Maryland	1978 - 1998
Research Associate, NASA/Goddard Institute for Space Studies	1976 - 1977
Assistant Professor of Atmospheric and Oceanic Science, State University of New York at Stony Brook	1975 - 1979

Refereed publications (last three years):

Gopalakrishnan, S.G., S. Goldenberg, T. Quirino, F. Marks, X. Zhang, K.-S. Yeh, R. Atlas, and V. Tallapragada, 2012: Towards improving high-resolution numerical hurricane forecasting: Influence of model horizontal grid resolution, initialization, and physics. *Weather and Forecasting*, 27 (3), 647-666.

Yeh, K.-S., X. Zhang, S.G. Gopalakrishnan, S. Aberson, R. Rogers, F.D. Marks, and R. Atlas, 2012: Performance of the experimental HWRF in the 2008 hurricane season. *Natural Hazards*, 63 (3), 1439-1449.

Hoffman, R.N., J.V. Ardizzone, S.M. Leidner, D.K. Smith, J.C. Jusem, and R.M. Atlas, 2013: Error estimates for ocean surface winds: Applying Desroziers diagnostics to the cross-calibrated, multi-platform analysis of wind speed. *Journal of Oceanic and Atmospheric Technology*, 30 (11), 2596-2603.

Lee, S.-K., D.B. Enfield, H. Liu, C. Wang, and R. Atlas, 2013: Is there an optimal ENSO pattern that enhances large-scale atmospheric processes conducive to major tornado outbreaks in the United States? *Journal of Climate*, 26 (5), 1626-1642.

Nolan, D.S., R. Atlas, K.T. Bhatia, and L.R. Bucci, 2013: Development and validation of a hurricane nature run using the joint OSSE nature run and the WRF model. *Journal of Advances in Modeling Earth Systems*, 5 (2), 382-405.

Prive N.C., Y. Xie, J. Woollen, S. Koch, R. Atlas, and R. Hood, 2013: Evaluation of the Earth Systems Research Laboratory (ESRL) global Observing System Simulation Experiment (OSSE) system. *Tellus A*, 65, 19011 (doi:10.3402/tellusa.v65i0.19011), 22 pp.

Ralph, F.M., J. Intrieri, D. Andra, R. Atlas, S. Boukabara, D. Bright, P. Davidson, B. Entwistle, J. Gaynor, S. Goodman, J.-G. Jiing, A. Harless, J. Huang, G. Jedlovec, J. Kain, S. Koch, B. Kuo, J. Levit, S. Murillo, L.P. Riishojgaard, T. Schneider, R. Schneider, T. Smith, and S.

Weiss, 2013: The emergence of weather-related testbeds linking research and forecasting operations. *Bulletin of the American Meteorological Society*, 94 (8), 1187-1211.

Baker, W.E., R. Atlas, C. Cardinali, A. Clement, G.D. Emmitt, B.M. Gentry, R.M. Hardesty, E. Kallen, M.J. Kavaya, R. Langland, M. Masutani, W. McCarty, R.B. Pierce, Z. Pu, L.P. Riishojgaard, J. Ryan, S. Tucker, M. Weissmann, and J.G. Yoe, 2014: Lidar-measured wind profiles: The missing link in the global observing system. *Bulletin of the American Meteorological Society*, 95 (4), 543-564.

Halliwell, G.R., A. Srinivasan, H. Yang, D. Willey, M. Le Henaff, V. Kourafalou, and R. Atlas, 2014: Rigorous evaluation of a fraternal twin ocean OSSE system for the open Gulf of Mexico. *Journal of Oceanic and Atmospheric Technology*, 31 (1), 105-130.

Prive, N.C., Y. Xie, S. Koch, R. Atlas, S.J. Majumdar, and R.N. Hoffman, 2014: An observing system simulation experiment for the unmanned aircraft system data impact on tropical cyclone track forecasts. *Monthly Weather Review* 142 (11), 4357-4363.

Halliwell, G.R., V. Kourafalou, M. Le Henaff, R. Atlas, and L.K. Shay, 2014: OSSE impact analysis of airborne ocean surveys for improving upper-ocean dynamical and thermodynamical forces in the Gulf of Mexico. *Progress in Oceanography* (In Press).

Five other publications:

Joiner, J., E. Brin, R. Treadon, J. Derber, P. Van Delst, A. Da Silva, J. Le Marshall, P. Poli, R. Atlas, D. Bungato, and C. Cruz, 2007. Effects of data selection and error specification on the assimilation of AIRS data. *Q. J. Roy. Meteor. Soc.*, 133, 181-196.

Chahine, M.T., T.S. Pagano, H.H. Aumann, R. Atlas, C. Barnet, J. Blaisdell, L. Chen, M. Divakarla, E.J. Fetzer, M. Goldberg, C. Gautier, S. Granger, S. Hannon, F.W. Irion, R. Kakar, E. Kalnay, B.H. Lambrigtsen, S.-Y. Lee, J. LeMarshall, W.W. McMillan, L. McMillin, E.T. Olsen, H. Revercomb, P. Rosenkranz,W.L. Smith, D. Staelin, L.L. Strow, J. Susskind, D. Tobin, W. Wolf, and L. Zhou. AIRS: Improving weather forecasting and providing new data on greenhouse gases, 2006. *B. Am. Meteorol. Soc.*, 87, 911-926.

Shen, B.-W., R. Atlas, J.-D. Chern, O. Reale, S.-J. Lin, T. Lee, and J. Chang, 2006. The 0.125 degree finite-volume general circulation model on the NASA Columbia supercomputer: Preliminary simulations of mesoscale vortices. *Geophys. Res. Lett.*, 33, L05801, doi:10.1029/2005GL024594.

Shen, B.-W., R. Atlas, O. Reale, S.-J. Lin, J.-D. Chern, J. Chang, C. Henze, and J.-L. Li. Hurricane forecasts with a global mesoscale-resolving model: Preliminary results with Hurricane Katrina (2005), 2006. *Geophys. Res. Lett.*, 33, L13813, doi:10.1029/2006GL026143.

Atlas, R., O. Reale, B.-W. Shen, S.-J. Lin, J.-D. Chern, W. Putman, T. Lee, K.-S. Yeh, M. Bosilovich, and J. Radakovich, 2005. Hurricane forecasting with the high-resolution NASA finite volume general circulation model. *Geophys. Res. Lett.*, 32, L03807, doi:10.1029/2004GL021513.

Curriculum Vitae: Chunzai Wang

NOAA Atlantic Oceanographic and Meteorological Laboratory
4301 Rickenbacker Causeway, Miami, FL 33149
Chunzai.Wang@noaa.gov

Education:

Ph.D., University of South Florida (Physical Oceanography)	1995
M.S., Oregon State University (Atmospheric Science)	1991
B.S., Ocean University of China, China, (Marine Meteorology)	1982

Professional Experience:

Oceanographer, NOAA Atlantic Oceanographic and Meteorological Laboratory	2000 - Present
Associate Scientist, CIMAS/RSMAS, University of Miami	1999 - 2000
Research Associate, College of Marine Science, University of South Florida	1997 - 1999
Postdoctoral Associate, College of Marine Science, University of South Florida	1995 - 1997

Service:

Co-chair, Intra-Americas Study of Climate Processes (IASCLIP) Program	2014 - Present
Editor, Journal of Geophysical Research (Oceans)	2009 – Present
Associate Editor, Journal of Climate	2006 – Present
American Geophysical Union Books Board	2005 – 2010

Recent Publications (last three years):

Zhang, L., C. Wang, Z. Song, and S.-K. Lee, 2014: Remote effect of the model cold bias in the tropical North Atlantic on the warm bias in the tropical Southeastern Pacific. *J. Adv. Model. Earth Syst.*, in press.

Ling, Z., G. Wang, and C. Wang, 2014: Out-of-phase relationship between tropical cyclones generated locally in the South China Sea and non-locally from the northwest Pacific Ocean. *Clim. Dyn.*, in press.

Yeh, S.-W., X. Wang, C. Wang, and B. Dewitte, 2014: On the relationship between the North Pacific climate variability and the Central Pacific El Niño. *J. Climate*, in press.

Yang, L., Y. Du, D. Wang, C. Wang, and X. Wang, 2014: Impact of intraseasonal oscillation on the tropical cyclone track in the South China Sea. *Clim. Dyn.*, in press.

Wang, X. D., C. Wang, G. Han, W. Li, and X. Wu, 2014: Effects of tropical cyclones on large-scale circulation and ocean heat transport in the South China Sea. *Clim. Dyn.*, in press.

Wang, C., C. Deser, J.-Y. Yu, P. DiNezio, and A. Clement, 2014: El Niño-Southern Oscillation (ENSO): A review. In *Coral Reefs of the Eastern Pacific*, P. Glymn, D. Manzello, and I. Enochs, Eds., Springer Science Publisher, in press.

Liu, H., C. Wang, S.-K. Lee, and D. B. Enfield, 2014: Inhomogeneous influence of the Atlantic warm pool on United States precipitation. *Atmos. Sci. Lett.*, in press.

Song, Z., H. Liu, L. Zhang, F. Qiao, and C. Wang, 2014: Evaluation of the eastern equatorial Pacific SST seasonal cycle in CMIP5 models. *Ocean Sci. Discuss.*, **11**, 1129-1147.

Li, Y., W. Han, T. Shinoda, C. Wang, M. Ravichandran, and J.-W. Wang, 2014: Revisiting the wintertime intraseasonal SST variability in the tropical South Indian Ocean: Impact of the ocean interannual variation. *J. Phys. Oceanogr.*, **44**, 1886-1907.

Wang, C., 2014: [The Tropics] Atlantic warm pool [in "State of the Climate in 2013"]. *Bull. Amer. Meteor. Soc.*, **95** (7), S105-S109.

Zhang, L., C. Wang, and S.-K. Lee, 2014: Potential role of Atlantic warm pool-induced freshwater forcing in the Atlantic meridional overturning circulation: Ocean-sea ice model simulations. *Clim. Dyn.*, **43**, 553-574.

Wang, W., X. Zhu, C. Wang, and A. Köhl, 2014: Deep meridional overturning circulation in the Indian Ocean and its relation to Indian Ocean dipole. *J. Climate*, **27**, 4508-4520.

Li, C. and C. Wang, 2014: Simulated impacts of two types of ENSO events on tropical cyclone activity in the western North Pacific: Large-scale atmospheric response. *Clim. Dyn.*, **42**, 2727–2743.

Lee, S.-K., B. E. Mapes, C. Wang, D. B. Enfield, and S. J. Weaver, 2014: Springtime ENSO phase evolution and its relation to rainfall in the continental U.S. *Geophys. Res. Lett.*, **41**, 1673–1680, doi:10.1002/2013GL059137.

Maloney, E. D., et al., 2014: North American climate in CMIP5 experiments: Part III: Assessment of 21st Century projections. *J. Climate*, **27**, 2230-2270.

Wang, C., L. Zhang, S.-K. Lee., L. Wu, and C. R. Mechoso, 2014: A global perspective on CMIP5 climate model biases. *Nature Climate Change*, **4**, 201-205.

Wang, X., and C. Wang, 2014: Different impacts of various El Niño events on the Indian Ocean dipole. *Climate Dynamics*, **42**, 991-1005, DOI 10.1007/s00382-013-1711-2.

Lee, S.-K., C. R. Mechoso, C. Wang, and J. D. Neelin, 2013: Interhemispheric influence of the northern summer monsoons on the southern subtropical anticyclones. *J. Climate*, **26**, 10193-10204.

Li, W., L. Li, M. Ting, Y. Deng, Y. Kushnir, Y. Liu, Y. Lu, C. Wang, and P. Zhang, 2013: Intensification of the Southern Hemisphere summertime subtropical anticyclones in a warming climate. *Geophys. Res. Lett.*, **40**, 5959–5964, doi:10.1002/2013GL058124.

Zhang, L., and C. Wang, 2013: Multidecadal North Atlantic sea surface temperature and Atlantic meridional overturning circulation variability in CMIP5 historical simulations. *J. Geophys. Res.*, **118**, 5772–5791, doi:10.1002/jgrc.20390.

Li, Y., W. Han, T. Shinoda, C. Wang, R.-C. Lien, J. N. Moum, J.-W. Wang, 2013: Effects of solar radiation diurnal cycle on the tropical Indian Ocean mixed layer variability during wintertime Madden-Julian Oscillation events. *J. Geophys. Res.*, **118**, 4945–4964, doi:10.1002/jgrc.20395.

Sheffield, J., et al., 2013: North American Climate in CMIP5 Experiments: Part II: Evaluation of historical simulations of intra-seasonal to decadal variability. *J. Climate*, **26** (23), 9247-9290.

Wang, C., and L. Zhang, 2013: Multidecadal ocean temperature and salinity variability in the tropical North Atlantic: Linking with the AMO, AMOC and subtropical cell. *J. Climate*, **26**, 6137-6162.

Liu, H., C. Wang, S.-K. Lee, and D. B. Enfield, 2013: Atlantic warm pool variability in the CMIP5 simulations. *J. Climate*, **26**, 5315-5336.

Wang, C., C. Li, M. Mu, and W. Duan, 2013: Seasonal modulations of different impacts of two types of ENSO events on tropical cyclone activity in the western North Pacific. *Climate Dynamics*, **40**, 2887-2902.

Shinoda, T., T. Jensen, M. Flatau, S. Chen, W. Han, and C. Wang, 2013: Large-scale oceanic variability associated with the Madden-Julian oscillation during the CINDY/DYNAMO field campaign from satellite observations. *Remote Sens.*, **5**, 2072-2092.

Wang, X., C. Wang, W. Zhou, L. Liu, and D. Wang, 2013: Remote influence of North Atlantic SST on the equatorial westerly wind anomalies in the western Pacific for initiating an El Niño event: An atmospheric general circulation model study. *Atmos. Sci. Lett.*, **14**, 107-111.

Zheng, J., Q. Liu, C. Wang, and X.-T. Zheng, 2013: Impact of heating anomalies associated with rainfall variations over the Indo-Western Pacific on Asian atmospheric circulation in winter. *Climate Dynamics*, **40**, 2023-2033.

Lee, S.-K., R. Atlas, D. B. Enfield, C. Wang, and H. Liu, 2013: Is there an optimal ENSO pattern that enhances large-scale atmospheric processes conducive to major tornado outbreaks in the U. S.? *J. Climate*, **26**, 1626-1642.

Wang, C., L. Zhang, and S.-K. Lee, 2013: Response of freshwater flux and sea surface salinity to variability of the Atlantic warm pool. *J. Climate*, **26**, 1249-1267.

Wang, C., and X. Wang, 2013: Classifying El Nino Modoki I and II by different impacts on rainfall in southern China and typhoon tracks. *J Climate*, **26**, 1322-1338.

Wang, X., W. Zhou, D. Wang, and C. Wang, 2013: The impacts of the summer Asian jet stream biases on surface air temperature in mid-eastern China in IPCC AR4 models. *Int'l J. Clim.*, **33**, 265-276.

Wang, G., J. Li, C. Wang, and Y. Yan, 2012: Interactions among the winter monsoon, ocean eddy and ocean thermal front in the South China Sea. *J. Geophys. Res.*, **117**, C08002, doi: 10.1029/2012JC008007.

Zhang, L., C. Wang, and L. Wu, 2012: Low-frequency modulation of the Atlantic warm pool by the Atlantic multidecadal oscillation. *Climate Dynamics*, **39**, 1661–1671.

Zhang, L., and C. Wang, 2012: Remote influences on freshwater flux variability in the Atlantic warm pool region. *Geophys. Res. Lett.*, **39**, L19714, doi:10.1029/2012GL053530.

Liu, H., C. Wang, S.-K. Lee, and D. B. Enfield, 2012: Atlantic warm pool variability in the IPCC AR4 CGCM simulations. *J. Climate*, **25**, 5612-5628.

Wang, C., 2012: Atlantic multidecadal oscillation (AMO) [in "State of the Climate in 2011"]. *Bull. Amer. Meteor. Soc.*, **93** (7), S119-S122.

Wang, C., S. Dong, A. T. Evan, G. R. Foltz, and S.-K. Lee, 2012: Multidecadal covariability of North Atlantic sea surface temperature, African dust, Sahel rainfall and Atlantic hurricanes. *J. Climate*, **25**, 5404-5415.

Larson, S., S.-K. Lee, C. Wang, E.-S. Chung, and D. Enfield, 2012: Impacts of non-canonical El Niño patterns on Atlantic hurricane activity. *Geophys. Res. Lett.*, **39**, L14706, doi:10.1029/2012GL052595.

Shu, Q., F. Qiao, Z. Song, and C. Wang, 2012: Sea ice trends in the Antarctic and their relationship to surface air temperature during 1979 to 2009. *Climate Dynamics*, **38**, 2355–2363.

Song, Z., F. Qiao, X. Lei, and C. Wang, 2012: Influence of parallel computational uncertainty on simulations of the coupled general climate model. *Geoscientific Model Development*, **5**, 313-319.

Li, W.-W., C. Wang, D. Wang, L. Yang and Y. Deng, 2012: Modulation of low-latitude west wind on abnormal track and intensity of tropical cyclone Nargis (2008) in the Bay of Bengal. *Adv. Atmos. Sci.*, 29, 407-421.

Curriculum Vitae: Scott J. Weaver
NOAA Climate Prediction Center
5830 University Research Court, College Park, MD 20740
Scott.Weaver@noaa.gov

Education:

Ph.D., University of Maryland (Atmospheric and Oceanic Science)	2007
M.S., University of Maryland (Atmospheric Science)	2003
B.S., Rutgers University (Meteorology)	2000

Professional Service:

NOAA Climate Prediction Center, Research Meteorologist	2009 - Present
NASA/GMAO, Postdoctoral Research Associate	2007 - 2009
Montgomery College, Adjunct Faculty	2007 - 2008
University of Maryland, Graduate Research Assistant	2001 - 2007
University of Maryland, Graduate Teaching Assistant	2001 - 2005
NRL, Solar Physics Branch, Research Assistant	2003 - 2007

Refereed publications (last three years):

Weaver, S. J., S. Baxter, and A. Kumar 2012: Climatic role of North American low-level jets on regional U.S. tornado activity. *J. Climate*, 25, 6666-6683.

Weaver, S. J., 2013: Factors associated with decadal variability in Great Plains summertime surface temperatures. *J. Climate*, 26, 343-350.

Kunkel, K., et al. (including S. J. Weaver), 2013: Monitoring and understanding changes in extreme storm statistics: state of knowledge. *Bull. Amer. Metor. Soc.*, 94, 499-514.

Liu, X., S. Yang, A. Kumar, S. J. Weaver, and X. Jiang, 2013: Diagnostics of sub-seasonal prediction biases of the Asian summer monsoon by the NCEP Climate Forecast System. *Climate Dyn*., 40, DOI: 10.1007/s00382-012-1553-3.

Liu, X, S. Yang, Q. Li, A. Kumar, S. J. Weaver, and S. Liu, 2013: Subseasonal forecast skills of global summer monsoons in the NCEP Climate Forecast System version 2. *Climate Dynamics*, 40, DOI: 10.1007/s00382-013-1831-8.

Wang, W., et al. (including S. J. Weaver), 2013: MJO prediction in the NCEP climate forecast system version 2. *Climate Dynamics*, DOI:10.1007/s00382-013-1806-9.

Fu, X. et al. (including S. J. Weaver), 2013: Multi-model MJO forecasting during DYNAMO/CINDY period. *Climate Dynamics*, 41, 1067-1081.

Hung, M-P, J-L Lin, W. Wang, D. Kim, T. Shinoda, and S. J Weaver, 2013: MJO and Convectively Coupled Equatorial Waves Simulated by CMIP5 Climate Models. *J. Climate*, 26, 6185-6214.

Weaver, S. J., and coauthors 2013: Advancing the Nation's capability to anticipate tornado and severe weather risk. *Non-peer reviewed white paper.* Available at: http://www.cpc.ncep.noaa.gov/products/severe_weather/Climate.Severe.Weather.White.Paper.Apr2013.pdf.

Weaver, S. J., and coauthors 2013: Tornadoes, climate variability, and climate change. National Oceanic and Atmospheric Administration state of the science fact sheet. Available at: http://nrc.noaa.gov/CouncilProducts/ScienceFactSheets.aspx.

Weaver, S. J., A. Kumar, and M. Chen, 2014: Recent increases in extreme temperature Occurrence over land. *Geophys. Res. Lett.*, 41, 4669–4675, doi:10.1002/2014GL060300.

Lee, S-K, B. E. Mapes, C. Wang, D. B. Enfield, and S. J. Weaver, 2014: Springtime ENSO phase evolution and its relation to rainfall in the continental U.S. *Geophys. Res. Lett.*, 41, 1673-1680, doi:10.1002/2013GL060300.

Baxter, S., S. J. Weaver, J. Gottschalck, and Y. Xue, 2014: Pentad Evolution of Wintertime Impacts of the Madden-Julian Oscillation Over the Contiguous United States. *J. Climate*. In-press.

Other five publications:

Weaver, S. J., and S. Nigam, 2008: Variability of the Great Plains low-level jet: Large scale circulation context and hydroclimate impacts. *J. Climate*. 21, 1532-1551.

Weaver, S. J., A. Ruiz-Barradas, and S. Nigam 2009: Pentad evolution of the 1988 drought and 1993 flood over the Great Plains: A NARR perspective on the atmospheric and terrestrial water balances. *J. Climate*, 22, 5366-5384.

Weaver, S. J., and S. Schubert, 2009: Warm season variations in the low-level circulation and precipitation over the central U.S. in observations, AMIP simulations, and idealized SST experiments. *J. Climate*, 22, 5401-5420.

Schubert, S. et al. (including S. J. Weaver), 2009: A US CLIVAR Project to assess and compare the responses of global climate models to drought-related SST forcing patterns: Overview and results, *J. Climate*, 22, 5251-5272.

Weaver, S. J., and S. Nigam, 2011: Recurrent supersynoptic evolution of the Great Plains low-level jet. *J. Climate*, 24, 575-582.

Current and Pending Support

Current:

(1) NOAA/CPO MAPP Program: Toward developing a seasonal outlook for the occurrence of major U. S. tornado outbreaks, PIs: S.-K. Lee (4 mon/yr), R. Atlas, C. Wang, D. B. Enfield, and S. Weaver, $430.0K, August 1, 2012 to July 31, 2015.

(2) NOAA/CPO MAPP Program: Variability and predictability of the Atlantic warm pool and its impacts on extreme events in North America, PIs: C. Wang, S.-K. Lee (5 mon/yr) and D. B. Enfield, $442.2K, August 1, 2012 to July 31, 2015.

(3) NASA: Management and conservation of Atlantic Bluefin Tuna (Thunnus Thynnus) and other highly migratory fish in the Gulf of Mexico under IPCC climate change scenarios: A study using regional climate and habitat models, PIs: M. A. Roffer, J. T. Lamkin, F. E. Muller-Karger, S.-K. Lee (1 mon/yr), B. A. Muhling, and G. J. Goni, $722K, 1 Sep 2011 – 31 Aug 2015.

Pending:

This proposal.

DUNS Number

The DUNS number is 152764007.

National Environmental Policy Act (NEPA)

There are no adverse environmental impacts associated with this research.